Absorption of Near-Fields through Hyperbolic Metamaterials with Finite Thickness

Caner Guclu [#1], Salvatore Campione [#2], Filippo Capolino [#3]

[#] *Department of Electrical Engineering and Computer Science, University of California Irvine*
4131 Engineering Hall, Irvine, CA, 92697 USA
[1] `cguclu@uci.edu`
[2] `scampion@uci.edu`
[3] `f.capolino@uci.edu`

Abstract—**We use spectral theory to analyze the radiation of elementary dipoles located close to homogeneous hyperbolic metamaterials (HMs) with finite thickness, focusing on the effect of losses in the HM. We show that for loss tangents (due to anisotropy) smaller than or equal to 10^{-1} the effect of the HM on dipole radiation is twofold: first, it induces an enhancement in the emitted power; second, most of this power is directed toward the HM itself. Then, we investigate the power scattered by a plasmonic nanosphere under plane wave incidence on top of a realistic multilayered HM with finite thickness. The multilayered HM, when homogenized, exhibits loss tangents of the same order of our previous analysis. We finally report that the multilayered HM enhances the nanosphere's scattered power, which is mainly directed toward the multilayered HM, in agreement with results relative to impressed dipoles.**

I. INTRODUCTION

Hyperbolic metamaterials (HMs) have been very recently at the center of studies for many applications including focusing with subwavelength resolution [1-7], negative refraction [8], absorption [9-12], enhancement of spontaneous emission [13-15], quantum and thermal emitters [16, 17]. A review of applications of HMs has been recently reported in [18]. In particular, a spectral theory approach [19] has been used in [12] to show that infinitely extended HMs are promising candidates for the absorption of near-fields. We show in this paper how losses affect the potential of a HM with finite thickness to absorb near-fields generated near its surface.

II. SPECTRAL THEORY: CALCULATION OF THE POWER EMITTED BY AN IMPRESSED DIPOLE

Assume to have a dipole $\mathbf{P} = p_x \hat{\mathbf{x}} \delta(\mathbf{r})$ polarized transverse to the z axis is in proximity of a grounded, homogeneous HM with finite thickness as depicted in Fig. 1. The transmission line formalism [12, 19] is used to calculate the power emitted by the dipole. This formulation is flexible because the spectral power redistribution in both TE and TM wave spectra can be independently decomposed into the power directed towards the bottom space (substrate) and the upper space (free space). The total power radiated by the dipole is evaluated using the spectral integrals given as

$$P_{\text{up,down}} = \frac{\omega^2 |p_x|^2}{8\pi} \int_0^{+\infty} p_{\text{up,down}}(k_t)\, dk_t, \quad (1)$$

where k_t is the transverse wavenumber and

$$p_{\text{up,down}} = \frac{\text{Re}\left[Y_{\text{up,down}}^{\text{TM}*}(k_t)\right]}{\left|Y_{\text{up}}^{\text{TM}}(k_t) + Y_{\text{down}}^{\text{TM}}(k_t)\right|^2} k_t \\ + \frac{\text{Re}\left[Y_{\text{up,down}}^{\text{TE}*}(k_t)\right]}{\left|Y_{\text{up}}^{\text{TE}}(k_t) + Y_{\text{down}}^{\text{TE}}(k_t)\right|^2} k_t \quad . \quad (2)$$

The details of formulation and methods for the evaluation of TE and TM admittances in (2) have recently been reported in [12]. In the following, we denote with P_{up} and P_{down} the dipole emitted power directed to the free space and to the substrate, respectively.
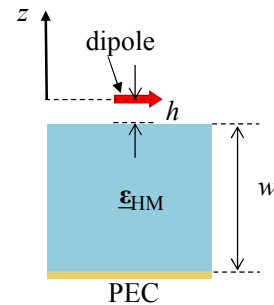

Fig. 1. An electric dipole polarized transverse to the z axis located at a distance h from the surface of a HM of finite thickness w.

III. EFFECT OF LOSSES ON REDISTRIBUTION OF POWER

It is well-known that the power emitted by dipoles in proximity of HMs experiences a dramatic increase due to the wide spatial spectrum of waves that can propagate inside HMs [12]. However, an increase in emitted power can also be achieved when the dipole is in proximity of an isotropic material with high losses. We thus believe it is important to determine a threshold of losses in HMs such that the composite HMs still preserve advantages versus a lossy isotropic material.

To this aim, we consider the two following substrates: (A) a homogeneous HM substrate characterized by a permittivity tensor $\underline{\varepsilon}_{\text{HM}} = \varepsilon_t (\hat{\mathbf{x}}\hat{\mathbf{x}} + \hat{\mathbf{y}}\hat{\mathbf{y}}) + \varepsilon_z \hat{\mathbf{z}}\hat{\mathbf{z}}$ whose entries are

$\varepsilon_t = \left(1 - j \tan \delta_t\right) \varepsilon_t'$ and $\varepsilon_z = \left(1 - j \tan \delta_z\right) \varepsilon_z'$ that results in a hyperbolic wave number dispersion for TM_z waves when $\varepsilon_t' \varepsilon_z' < 0$, as can be observed in Fig. 2 for a specific set of parameters; (B) a lossy dielectric with relative permittivity $\varepsilon_{\mathrm{die}} = \left(1 - j \tan \delta_{\mathrm{die}}\right) \varepsilon_{\mathrm{die}}'$.
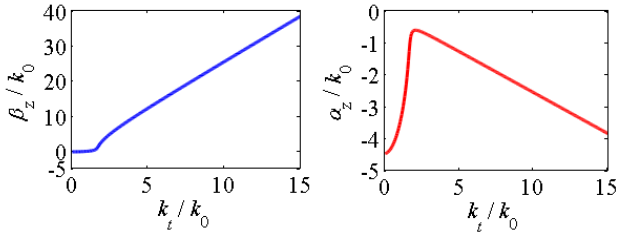
Fig. 2. Dispersion diagram of the homogeneous HM with $\varepsilon_t' = -20$, $\varepsilon_z' = 3$, and $\tan \delta_z = -\tan \delta_t = 0.1$ at frequency f_0.

As an example, we assume $\varepsilon_t' = -20$, $\varepsilon_z' = 3$, $\varepsilon_{\mathrm{die}}' = 4$, $h = \lambda_0 / 40$ and $w = \lambda_0 / 4$ where λ_0 is the wavenumber in free space at f_0. Then, we compute the total power $P_{\mathrm{tot}} = P_{\mathrm{up}} + P_{\mathrm{down}}$ emitted by the dipole and the ratio $P_{\mathrm{down}} / P_{\mathrm{up}}$ for various sets of $\tan \delta_t$, $\tan \delta_z$, and $\tan \delta_{\mathrm{die}}$ using (1).

In Fig. 3 we show an illustrative example. We plot P_{tot} (normalized by $P_{\mathrm{free\ space}}$, the power radiated by the same dipole in free space) versus $\left|\tan \delta_t\right| \in \left[10^{-4}, 1\right]$ (note that $\tan \delta_t < 0$ because $\varepsilon_t' < 0$) for four representative cases: HM substrates with (i) $\tan \delta_z = -0.1 \tan \delta_t$, (ii) $\tan \delta_z = -\tan \delta_t$, (iii) $\tan \delta_z = -10 \tan \delta_t$, and (iv) isotropic dielectric with $\tan \delta_{\mathrm{die}} = -\tan \delta_t$. When losses are comparable to the ones found in standard dielectrics ($\left|\tan \delta_t\right| \approx 10^{-2}$), the HM substrates [cases (i)-(iii)] enhance the radiated power by the dipole with a factor of ≈ 11.9 with respect to the dipole's radiation in free space, whereas for the dielectric substrate [case (iv)] the factor is only ≈ 1.7. However, as losses are increased, the power emitted by the dipole located above the dielectric substrate also increases. In particular, above $\left|\tan \delta_t\right| \approx 0.32$, it surpasses case (iii) and above $\left|\tan \delta_t\right| \approx 0.71$ it also surpasses cases (i)-(ii).

In Fig. 4, we plot the ratio $P_{\mathrm{down}} / P_{\mathrm{up}}$ for the same cases shown in Fig. 3. Analogously to the cases shown therein, we again observe that if losses are small, the use of HM substrates leads to a significant ratio $P_{\mathrm{down}} / P_{\mathrm{up}} \approx 80$, much larger than in the case of an isotropic dielectric, where $P_{\mathrm{down}} / P_{\mathrm{up}} \approx 3.5$; note however that the latter induces larger ratios for larger losses.
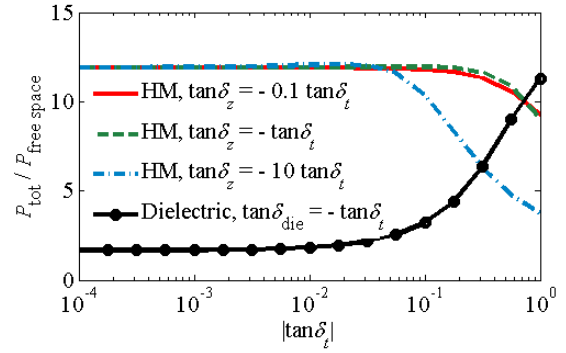
Fig. 3. Emitted power P_{tot} normalized by $P_{\mathrm{free\ space}}$ versus $\tan \delta_t$ for three homogeneous HMs and an isotropic dielectric at frequency f_0.
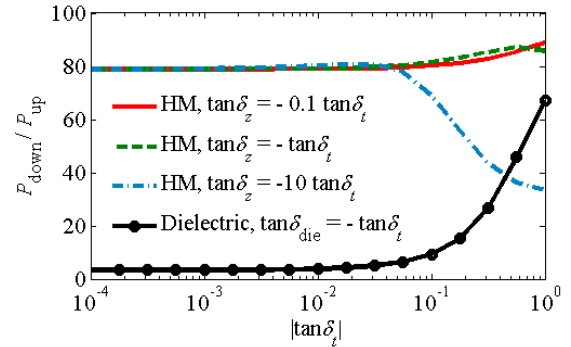
Fig. 4. Ratio $P_{\mathrm{down}} / P_{\mathrm{up}}$ versus $\tan \delta_t$ for three homogeneous HMs and an isotropic dielectric at frequency f_0.

IV. ENHANCEMENT AND ABSORPTION OF SCATTERED FIELDS IN PRESENCE OF HYPERBOLIC METAMATERIALS WITH FINITE THICKNESS

The plots in Fig. 3 and Fig. 4 have shown how losses in HMs affect the radiation of an impressed dipole. We then investigate the realistic scenario of near-field (generated by a scatterer under plane wave incidence) absorption by multilayered HMs.
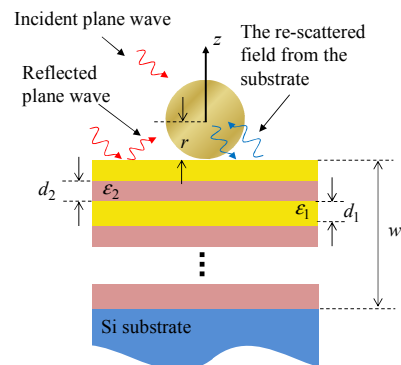
Fig. 5. A nanosphere with radius r located in proximity of a multilayered HM made of gold and alumina layers with thicknesses $d_1 = d_2 = 20\,\mathrm{nm}$. We consider 5 periods, so the total thickness of the HM substrate is $w = 200\,\mathrm{nm}$.

We consider a plasmonic nanosphere, here modelled as an electric dipole, on top of a multilayered HM, as illustrated in Fig. 5, which also shows all the scattering processes taken into account in our computation. In particular, the local field acting on the nanosphere accounts for the incident plane wave, the reflected plane wave from the substrate, and the self-coupling of the scattered field by the nanosphere through the substrate. The HM is composed of periodic layers of gold (whose permittivity is taken from [20]) and alumina with thicknesses $d_1 = d_2 = 20\,\text{nm}$. The HM under investigation has a finite thickness $w = 5(d_1 + d_2) = 200\,\text{nm}$ and is placed on top of a silicon substrate. The nanosphere is made of gold and has a radius $r = 20\,\text{nm}$.

In Fig. 6 we report (a) the real parts of the permittivity tensor entries and (b) the loss tangents obtained by effective medium approach [6, 12, 21] whose limitations have been recently discussed in [12, 21]. It is clear from Fig. 6(a) that the multilayered HM yields $\text{Re}(\varepsilon_t) < 0$ and $\text{Re}(\varepsilon_z) > 0$ over a very wide frequency band, guaranteeing hyperbolic wavenumber dispersion.
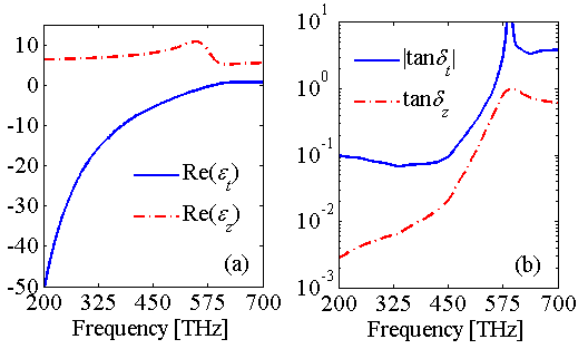

Fig. 6. (a) $\text{Re}(\varepsilon_t)$ and $\text{Re}(\varepsilon_z)$ for the homogenized version of the multilayered HM in Fig. 5. (b) Loss tangents $|\tan\delta_t|$ and $\tan\delta_z$ for the same case.
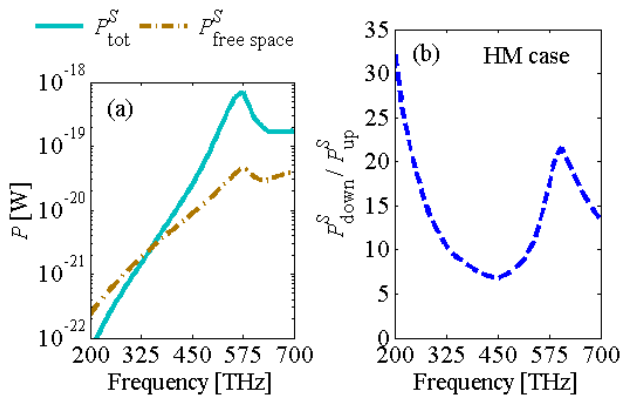

Fig. 7. (a) Nanosphere's total scattered power P_{tot}^S versus frequency in the case of a multilayered HM as in Fig. 5. The total scattered power $P_{\text{free space}}^S$ when the nanosphere is embedded in free space is also reported for comparison. (b) The ratio $P_{\text{down}}^S / P_{\text{up}}^S$ for the same HM case.

We now analyse the power scattered by the nanosphere relative to the multilayered HM in Fig. 5, computed again using (1) following the steps detailed in [12]. In Fig. 7(a), the total power $P_{\text{tot}}^S = P_{\text{up}}^S + P_{\text{down}}^S$ scattered by the nanosphere on top of the HM is plotted for normal plane wave incidence with $|\mathbf{E}| = 1\,\text{V/m}$. For comparison, we also plot the total power $P_{\text{free space}}^S$ scattered by the nanosphere when it is in free space. It should be noted that in the low frequency region of the plot (up to 360 THz) in Fig. 7(a), the HM does not provide an enhancement of the scattered power. Above 360 THz, we observe $P_{\text{tot}}^S > P_{\text{free space}}^S$. At around 580 THz, we observe a peak for both cases, although the scattered power in the HM case is as large as $P_{\text{tot}}^S \approx 15 P_{\text{free space}}^S$. In Fig. 6(b) we observe that from 360 THz up to 500 THz, both $|\tan\delta_t|$ and $\tan\delta_z$ are around 0.1, and from 500 THz up to 590 THz the loss tangents of the HM grow rapidly where $|\tan\delta_t|$ becomes much larger than $\tan\delta_z$. However, we see that the enhancement of the scattered power [Fig. 7(a)] is preserved even for large $|\tan\delta_t|$, which is in agreement with the results in Fig. 3 (solid red curve for $\tan\delta_z = -0.1\tan\delta_t$). The ratio $P_{\text{down}}^S / P_{\text{up}}^S$ is reported in Fig. 7(b) for the HM case in Fig. 7(a). We observe that independent of tangent loss levels in Fig. 6(b), most of the scattered power is directed towards the multilayered HM substrate in agreement with the results in Fig. 4. Moreover, we note that even though in the low frequency region of the plot the scattered power is not enhanced with respect to the free space case [Fig. 7(a)], most of this power is directed toward the HM as outlined in Fig. 7(b).

V. CONCLUSION

The results shown in this paper inherently show that HMs can be used as an innovative way to absorb near-fields: when they are coupled to the HM, they are transformed into propagating spectral components with very large wavenumbers. In particular, we have observed that (i) multilayered HMs enhance the amount of power scattered by a nanosphere in close proximity to the HM surface. Moreover, (ii) the scattered power is mostly redistributed toward the HM substrate. We observe that HMs preserve these qualities when the homogeneous permittivity tensor entries exhibit loss tangents up to about 0.1.

REFERENCES

[1] J. B. Pendry and S. A. Ramakrishna, "Refining the perfect lens," *Physica B-Condensed Matter,* vol. 338, pp. 329-332, Oct 2003.

[2] K. J. Webb and M. Yang, "Subwavelength imaging with a multilayer silver film structure," *Optics Letters,* vol. 31, pp. 2130-2132, Jul 2006.

[3] X. Li and F. Zhuang, "Multilayered structures with high subwavelength resolution based on the metal-dielectric composites," *Journal of the Optical Society of America a-Optics Image Science and Vision,* vol. 26, pp. 2521-2525, Dec 2009.

[4] Y. Jin, "Improving subwavelength resolution of multilayered structures containing negative-permittivity layers by flatting the transmission

curves," *Progress in Electromagnetics Research-Pier,* vol. 105, pp. 347-364, 2010.

[5] C. Della Giovampaola, M. Albani, and F. Capolino, "Investigation on subwavelength focusing properties of metal-dielectric multilayer," in *Metamaterials Congress, Barcelona, Spain, October 10-15, 2011,* 2011.

[6] R. Kotyński, T. Stefaniuk, and A. Pastuszczak, "Sub-wavelength diffraction-free imaging with low-loss metal-dielectric multilayers," *Applied Physics A: Materials Science & Processing,* vol. 103, pp. 905-909, 2011.

[7] Z. Liu, Z. Liang, X. Jiang, X. Hu, X. Li, and J. Zi, "Hyper-interface, the bridge between radiative wave and evanescent wave," *Applied Physics Letters,* vol. 96, pp. 113507-3, 2010.

[8] G. V. Naik, J. Liu, A. V. Kildishev, V. M. Shalaev, and A. Boltasseva, "Demonstration of Al:ZnO as a plasmonic component for near-infrared metamaterials," *Proceedings of the National Academy of Sciences,* May 18, 2012 2012.

[9] T. U. Tumkur, L. Gu, J. K. Kitur, E. E. Narimanov, and M. A. Noginov, "Control of absorption with hyperbolic metamaterials," *Applied Physics Letters,* vol. 100, p. 161103, 2012.

[10] E. E. Narimanov, H. Li, Y. A. Barnakov, T. U. Tumkur, and M. A. Noginov, "Darker than black: radiation-absorbing metamaterial," *arXiv:1109.5469v1,* 2011.

[11] T. U. Tumkur, J. K. Kitur, B. Chu, L. Gu, V. A. Podolskiy, E. E. Narimanov, and M. A. Noginov, "Control of reflectance and transmittance in scattering and curvilinear hyperbolic metamaterials," *Applied Physics Letters,* vol. 101, pp. 091105-4, 2012.

[12] C. Guclu, S. Campione, and F. Capolino, "Hyperbolic metamaterial as super absorber for scattered fields generated at its surface," *Physical Review B,* vol. 86, p. 205130, 2012.

[13] X. Ni, G. Naik, A. Kildishev, Y. Barnakov, A. Boltasseva, and V. Shalaev, "Effect of metallic and hyperbolic metamaterial surfaces on electric and magnetic dipole emission transitions," *Applied Physics B: Lasers and Optics,* vol. 103, pp. 553-558, 2011.

[14] H. N. S. Krishnamoorthy, Z. Jacob, E. Narimanov, I. Kretzschmar, and V. M. Menon, "Topological Transitions in Metamaterials," *Science,* vol. 336, pp. 205-209, April 13, 2012 2012.

[15] A. N. Poddubny, P. A. Belov, P. Ginzburg, A. V. Zayats, and Y. S. Kivshar, "Microscopic model of Purcell enhancement in hyperbolic metamaterials," *Physical Review B,* vol. 86, p. 035148, 2012.

[16] Z. Jacob, "Quantum plasmonics," *Mrs Bulletin,* vol. 37, pp. 761-767, Aug 2012.

[17] S. A. Biehs, M. Tschikin, and P. Ben-Abdallah, "Hyperbolic Metamaterials as an Analog of a Blackbody in the Near Field," *Physical Review Letters,* vol. 109, p. 104301, 2012.

[18] C. L. Cortes, W. Newman, S. Molesky, and Z. Jacob, "Quantum nanophotonics using hyperbolic metamaterials," *Journal of Optics,* vol. 14, p. 063001, 2012.

[19] L. B. Felsen and N. Marcuvitz, *Radiation and Scattering of Waves*: Prentice-Hall, NJ, 1973.

[20] P. B. Johnson and R. W. Christy, "Optical Constants of the Noble Metals," *Physical Review B,* vol. 6, pp. 4370-4379, 1972.

[21] O. Kidwai, S. V. Zhukovsky, and J. E. Sipe, "Dipole radiation near hyperbolic metamaterials: applicability of effective-medium approximation," *Optics Letters,* vol. 36, pp. 2530-2532, 2011.